Journal of Alloys and Compounds 663 (2016) 100–106

Contents lists available at ScienceDirect

Journal of Alloys and Compounds

journal homepage: http://www.elsevier.com/locate/jalcom

Half metallicity and magnetism in graphene containing monovacancies decorated with Carbon/Nitrogen adatom

Jyoti Thakur [a], Manish K. Kashyap [a, *], Hardev S. Saini [b], Ali H. Reshak [c, d]

[a] Department of Physics, Kurukshetra University, Kurukshetra, 136119, Haryana, India
[b] Department of Physics, Panjab University, Chandigarh, 160014, India
[c] New Technologies – Research Centre, University of West Bohemia, Univerzitni 8, 306 14, Pilsen, Czech Republic
[d] Center of Excellence Geopolymer and Green Technology, School of Material Engineering, University Malaysia Perlis, 01007, Kangar, Perlis, Malaysia

ARTICLE INFO

Article history:
Received 15 November 2015
Received in revised form
10 December 2015
Accepted 15 December 2015
Available online 18 December 2015

Keywords:
DFT
FPLAPW
Spintronics
Graphene

ABSTRACT

It is an important issue to induce the magnetic channel and band gap in pristine graphene by creating monovacancies. However, the graphene containing monovacancies is not found to be truly half metallic. The tuning of its electronic properties via C/N-adsorption has been investigated using the first-principles density functional theory (DFT) calculations, with the aims to achieve 100% spin-polarization and enhanced magnetism. C/N-adsorption generates half metallicity in graphene containing monovacancies and magnetic moment is found to be almost double/triple as compared to case of monovacancies only. The origin of magnetism has been identified via interaction of p-states of adsorbed atom with p-states of inequivalent C-atoms present in the vicinity of adsorption site. Our results indicate that the surface adsorption of C/N is a promising approach to enhance the potential of graphene in future spintronic and magnetic device applications.

1. Introduction

Graphene, a two-dimensional (2D) single layer of C-atoms arranged in a honeycomb lattice, is in limelight since its first synthesis by Novoselov and co-workers in 2004 [1]. It has unique zero-gap electronic structure and possesses massless Dirac fermionic behavior. The unusual electronic and structural properties make it a prospective substitute material for "beyond-Si electronics" [2–6]. Manipulating the novel properties of graphene, such as carrier concentration and magnetism by incorporating defects is an important area of research for the deployment of graphene in spintronic and magnetic devices [7–16].

Pristine graphene sheet is semi-metallic and non-magnetic; however, the magnetism can be induced in graphene either by creating vacancy defect or by doping transition metal atoms [17–28]. The existence of different types of defects has also been proved experimentally [29,30]. These defects can easily be created by electric field [31–33], absorption of adatoms during sample preparation, ion irradiations [34–37] and edge modification [38–41]. The experimental synthesis may also include the formation of defects/disorders [42]; therefore vacancy mediated physical changes may appear in the materials. A direct evidence for ferromagnetic ordering locally at defect structures in highly oriented pyrolytic graphite observed by magnetic force microscopy is available [43]; the observed room temperature ferromagnetism gets appeared due to the presence of unpaired electron spins localized at grain boundaries.

Theoretically, it is an important aspect to reveal the role of defects or vacancies in the materials for simulating the real experimental observations. To understand the experimental observation of ferromagnetism in graphite samples by proton irradiation, spin polarized DFT calculations of magnetic properties of defects which are most likely to appear by irradiating graphite to form vacancies and vacancies Hydrogen complexes, have been performed [44]. It is observed that both defects are magnetic but latter one gives rise to magnetic moment double that of naked vacancy. Further, the graphene structure containing two separated single vacancies [45] shows a magnetic moment of 1.09 μ_B/vacancy. The magnetic moment of graphene containing monovacancies (G-MV) in the range, 1.12–1.53 μ_B, depending on vacancy concentration is also reported [46]. Moreover, the stability and electronic properties of the vacancy defect and F-adsorbed vacancy on graphene have also been studied extensively [47]. It is found that the local magnetic

* Corresponding author.
E-mail addresses: manishdft@gmail.com, mkumar@kuk.ac.in (M.K. Kashyap).

http://dx.doi.org/10.1016/j.jallcom.2015.12.117
0925-8388/

moment of graphene remains intact for odd number of F-adsorptions but gets destroyed for even F-adsorptions.

High spin-polarization and preferably half metallicity is the major quality of a material to be used in spintronic applications [7–9]. Though some papers deal with adsorption of atoms in pristine graphene [20,26,43] and F-adsorption in G-MV [47], but the reports on C and N atom adsorption in it are still missing. To extend the potential of graphene in spintronics by surface modification, we have targeted the G-MV nanomaterial in which non-metallic atom (C or N) has been adsorbed in the vicinity of monovacancies. The other aim of the present investigation is to check the effect of electro negativity of adsorbed atom on resultant magnetism in present nanosystems.

2. Computational details

The G-MV nanosheet with and without X-adsorption (X = C and N) were simulated by constructing $4 \times 4 \times 1$ supercell of graphene. This supercell is sufficient to simulate ~3% adsorption. A vacuum layer of 20 Å thickness in the z-direction was inserted to avoid the interlayer interaction due to periodic boundary conditions. We employed density functional theory (DFT) [48] based projected augmented wave (PAW) method as implemented in VASP [49,50] for the relaxation of the systems under investigation. The generalized gradient approximation (GGA) under Perdew–Burke–Ernzerhof parameterization was used to construct exchange-correlation potentials [51]. The PAW method is an all electron description and is used to describe the electron-ion description. The cutoff energy for plane-waves was set to be 500 eV, a $9 \times 9 \times 1$ Monkhorst-Pack grid was used for the sampling of the Brillouin zone during geometrical optimization. All the internal coordinates were allowed to be relaxed until calculated Hellmann Feynman force on each atom became smaller than 0.02 eV $Å^{-1}$.

We performed electronic structure calculations using the full-potential linearized augmented plane-wave (FPLAPW) [52] method within GGA as implemented in WIEN2k package [53]. In FPLAPW calculations, the core states were treated fully relativistically, whereas for the valence states, a scalar relativistic approach was used. Additionally, valence electronic wave functions inside the Muffin-tin sphere were expanded upto $l_{max} = 10$. The radii of the Muffin-tin sphere (R_{MT}) for various atoms were taken in the present calculations such as to ensure the nearly touching sphere. The plane-wave cutoff parameters were decided by $R_{mt} k_{max} = 7$ (where k_{max} is the largest wave vector of the basis set) and $G_{max} = 12$ a.u.$^{-1}$ for fourier expansion of potential in the interstitial region. The k-space integration was carried out using the modified tetrahedron method [54] with a k-mesh of $11 \times 11 \times 1$ for the high resolution in the calculations.

3. Result and discussion

The real experimental synthesis may contain the disorder/defect including vacancies and due to environmental contamination, these vacancies may adsorb a light electronegative atom (C/N) [55]. Thus the theoretical analysis of C/N-adsorbed G-MV is of prime importance. However, in order to find out the stable configuration for C/N-adsorbed graphene, various possible types of adsorption/doping were considered as shown in Fig. 1. For example, N-adsorption can have three possibilities; N atom is present (a) at the middle of two C-atoms surrounding vacancy, (b) acts as vacancy substitution and (c) is anchored with any of C-atoms nearby the vacancy (see, Fig. 1 (a), (b) and (c)). In case of C-adsorption, only (a) and (c) configurations are possible. On the basis of equilibrium energies (mentioned in Fig. 1), it is found that C/N-adsorption is most stable in (c) configuration. Hence, we have carried out the ground state properties of C/N-adsorbed G-MV in this case only.

The setup of the C/N-adsorbed graphene was considered as follows: In the first step, the monovacancies were created and then an electronegative atom C/N was adsorbed on anyone of C-atom in the vicinity of each monovacancy. The proposed supercells for G-MV and C/N-adsorbed G-MV were allowed to relax within PAW method in order to mediate any change in the atomic positions of various C-atoms and the C–C bond lengths of graphene. The layouts of graphene monolayer in pristine form, with monovacancies and on C/N-adsorption including monovacancies are depicted in Fig. 2. We believe that our results for the C–C bond lengths (as labeled in Fig. 2) in this study are accurate enough to simulate the exact experimental findings.

In pristine graphene, the C–C bond length is found to be 1.42 Å which agrees well with the previous report [56]. However, on creating monovacancies, the nearby C-atoms become non-equivalent and possess dangling bonds. The reduced structure gets relaxed by enlargement of the C–C bond lengths in the vicinity of monovacancies. On the other hand, the C-atoms away from monovacancies keep their original C–C bond lengths as in pristine case. This observation is in accordance with previous studies [22,23]. After C/N-adsorption at C_3 atom (Fig. 2), negligible change in all the C–C bond lengths is observed as compared to that in G-MV, which is also case for the B doped G-MV [57,58]. But C and N adsorption in G-MV yield bond length for C–C_{ads} as 1.170 Å and C–N_{ads} as 2.154 Å, respectively. The C_{ads} atom comes more close to graphene plane as compared N_{ads} atom, due to less electronegativity.

The formation energies for G-MV (E_{for}^{G-MV}) and C/N-adsorbed G-MV ($E_{for}^{C/N}$) can be estimated as under:

$$E_{for}^{G-MV} = E_{tot}^{G-MV} - E_{tot}^{pris} + E_{iso}^{C} \quad (1)$$

$$E_{for}^{C/N} = E_{tot}^{C/N} - E_{tot}^{G-MV} - E_{iso}^{C/N} \quad (2)$$

where E_{tot}^{pris}, E_{tot}^{G-MV} and $E_{tot}^{C/N}$ represent the total energy per unit atom of pristine graphene, G-MV and C/N-adsorbed G-MV, respectively. $E_{iso}^{C/N}$ denotes the energy of isolated Carbon/Nitrogen atom. The formation energy per unit atom of G-MV is found to be 6.92 eV, which is close to experimental value of 7.7 ± 0.5 eV [59], whereas on C/N absorption, its value becomes 7.85 eV/7.24 eV as mentioned in Table 1. The significant bond angles the adsorption site are also mentioned in this table. The bond angle (C_4–C_3–C_5 = 120°) of hexagonal symmetry in pristine graphene shows small deviation on creating monovacancies and further adsorption.

Before understanding the effect of C/N-adsorption in G-MV, it is an important to check the effect of vacancy on electronic properties of graphene. In this direction, we have compared spin polarized density of states (DOS) of pristine graphene and G-MV in Fig. 3. It has been found that monovacancies generate spin polarized DOS in the vicinity of the E_F to overcome the zero band gap of graphene and opens up a magnetic channel inside the graphene. Monovacancy i.e. removal of one C-atom in graphene leaves each of three neighboring C-atoms with sp^2 dangling bonds (unsatisfied valence electron on an immobilized C-atom). Two of these dangling bonds, say for C_1 and C_2 in Fig. 2(b) may be saturated by mutual sharing of electrons in the form of pentagon structure. These findings are in well agreement with the previously reported similar studies [60–62]. However, the third dangling bond on atom C_3 remains unsaturated which leads to the spin-polarization in G-MV. The spin-polarization (P) [63–65] as calculated by,

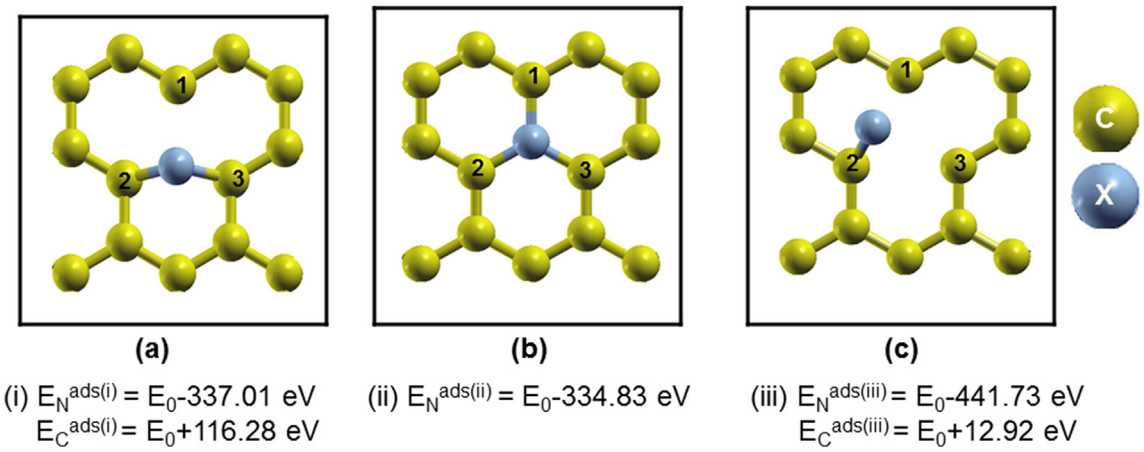

Fig. 1. G-MV on X-adsorption (X = C/N) in three configurations; (a) X is at the middle of two C-atoms surrounding vacancy, (b) X presents as vacancy substitute and (c) X is anchored with any of C-atoms nearby the vacancy. E_0 represents the equilibrium energy of pristine graphene.

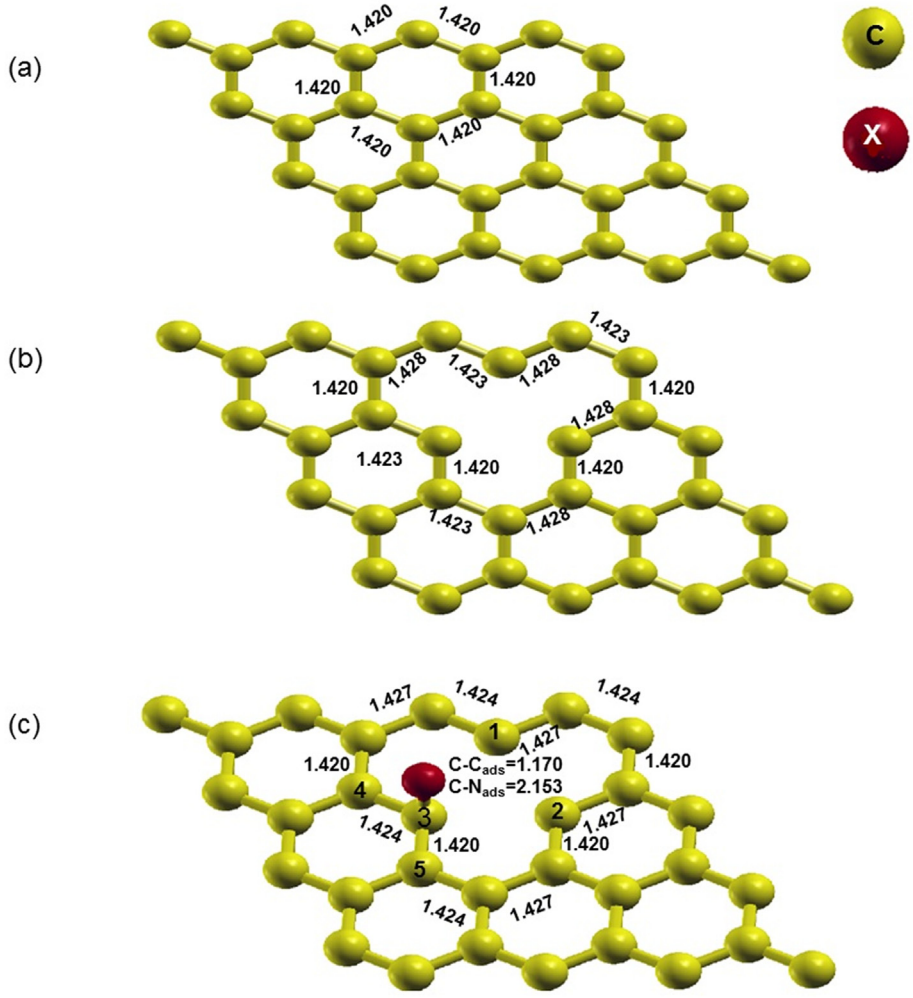

Fig. 2. The supercell arrangements of graphene (a) in pristine form, (b) containing monovacancies and (c) with both monovacancies and X-adsorption (X = C/N). The observed C–C bond lengths (Å) for relaxed structures in these forms are also mentioned.

$$P = \frac{N_{\uparrow}(E_F) - N_{\downarrow}(E_F)}{N_{\uparrow}(E_F) + N_{\downarrow}(E_F)} \quad (3)$$

where $N_{\uparrow}(E_F)$ and $N_{\downarrow}(E_F)$ are the spin dependent DOS of majority (MAC) and minority (MIC) spin channels at E_F, respectively, is found to be only 50% in G-MV. It is interested to note that with mono-vacancies, both the spin channels of graphene become metallic

Table 1
Calculated bond angles (in degree) and formation energies; E_{For} (in eV) of pristine graphene, G-MV and C/N-adsorbed G-MV.

Graphene	Bond angles			E_{For}
	$X–C_3$-C_4	$X–C_3$-C_5	$C_3–C_4–C_5$	
Pristine case	–	–	120.00	–
G-MV	–	–	119.98	−6.92
C-adsorbed G-MV	51.37	101.21	119.76	−7.85
N-adsorbed G-MV	57.04	96.06	119.76	−7.24

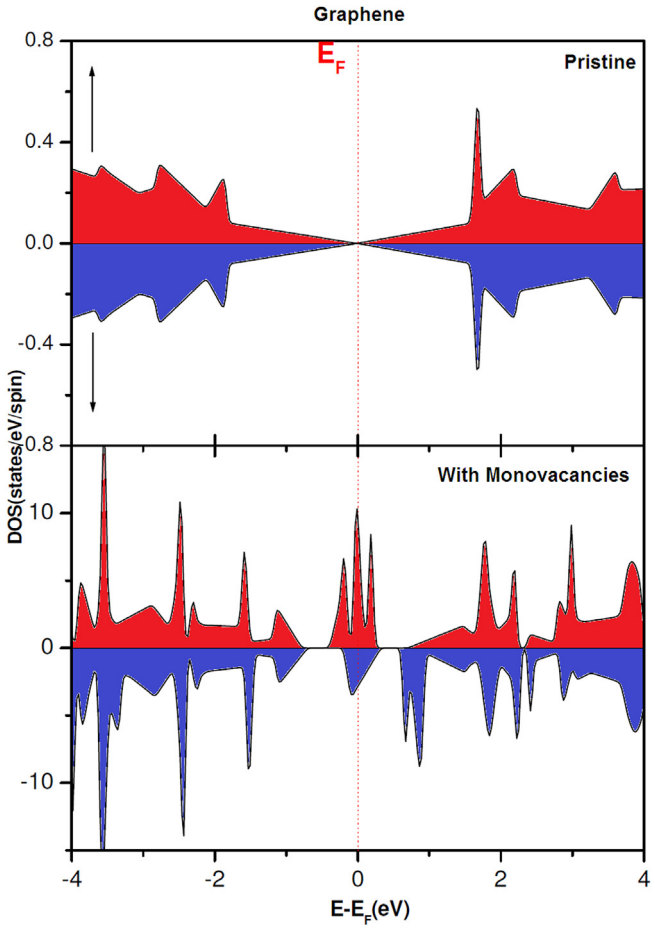

Fig. 3. Total spin polarized density of states (TDOS) of graphene in pristine form and containing monovacancies.

which were semiconducting with zero band gaps in pristine case [66].

After understanding nature of G-MV, C/N-adsorption in proposed 4 × 4 × 1 supercell of graphene has been studied in it by exploiting the total and partial DOS for each adsorption in Fig. 4. The adsorbed atom in G-MV is very crucial to decide the spin-polarization and magnetism. C/N-adsorption in G-MV enhances the spin-polarization (P) at E_F from 50 to 100% (Table 2) and makes the resultant nanomaterials as truly half metallic. While sharing one electron at adsorption site with C-atom of graphene sheet, the adsorbed C/N atom also keeps unpaired electrons with it. On checking the right panel of Fig. 4, it is confirmed that C-p/N-p-states of adsorbed atom are available for conduction in the vicinity of the E_F. Further C-s/N-s states are negligible near E_F, which justifies that only π-orbitals of adsorbed atom are mainly responsible for the spin-polarization. The high degree of the spin-polarization ensures that the passage of large amount of preferred spin current and thus, these nanomaterials may be suitable for spin filter devices [67–69]. In order to ensure the right prediction of half metallicity, the ground state calculations were performed and cross checked for heavier supercells as well e.g. 7 × 7 × 1 and 8 × 8 × 1. However, no qualitative changes in DOS have been noticed as that in 4 × 4 × 1. Thus we kept the same 4 × 4 × 1 supercell for time efficient calculations. The suitability of small 4 × 4 × 1 or 5 × 5 × 1 supercell for addressing the monovacancies has been justified previously as well [47,70,71]. An appreciable band gap of 0.71 eV/0.62 eV has been observed in MIC on C/N-adsorption in graphene which can lead to interesting optical properties. Indeed, there exist few reports which support our observation completely [72,73].

The existence of the HM gap i.e., a minimal gap for spin excitation in MIC is a striking feature of a material. This gap is of unique importance for creating a hole and electron in MIC. It is defined as minimum of difference between E_F and E_v^{top} or E_F and E_c^{bot} where E_v^{top} and E_c^{bot} represent the energy corresponding to top of valence band (VB) and bottom of conduction band (CB) in MIC, respectively. A true HM Ferro magnet is governed by a non zero HM gap instead of band gap in any spin channel [74,75]. Thus, it is to be calculated for clear understanding of half metallicity of the material, Table 2 also manifests the HM gap and energy band gap in MIC of resultant systems. C-adsorption results zero HM gap, whereas for N-adsorption its value is 0.1 eV. Almost zero HM gap in both adsorption manifests that no threshold energy is required to move electron from occupied states to empty states in present nanomaterials and due to this, excellent spin transport properties may be observed in these [76–79]. The adsorption in G-MV influences C-atoms present nearby to adsorption site and make them non-equivalent. It is important to check how the electronic states of these C-atoms are varying with adsorption. To analyze the same, we present their DOS along with accumulated TDOS of C-adsorbed G-MV in Fig. 5. The similar explanation may be drawn for N-adsorption also.

It is found that total DOS of C-adsorbed G-MV has main contribution not only from adsorbed C-atoms but also from nearby inequivalent C-atoms (C_1, C_2 and C_3). Due to adsorption, the p-states of adsorbed C-atoms interact with p-states of C_1, C_2 and C_3 atoms effectively and polarized their DOS significantly. This polarization is highly visible in the vicinity of the E_F which leads to generate half metallicity in the resultant nanomaterials. Various states in MIC are easily available for conduction now in the vicinity of E_F and spin polarized current can flow by small excitation only. The nearby C-atoms also play significant role in the spin conduction as they strengthen the DOS in CB of MIC along with adsorbed C-atoms (C_{ads}). Though, other C-atoms also have polarized DOS but its significant amount is present only at high energy (away from E_F), thus their contribution can be ruled out for easy spin conduction. For example, the DOS for one C-atom (C_{far}) far away from adsorption site is shown in last panel of Fig. 5, but the DOS for this atom is negligible in the vicinity of the E_F.

Pristine graphene has zero magnetic moment whereas on creating monovacancies, due to difference in the DOS of electrons in MAC and MIC, a magnetic moment of 0.99 μ_B gets induced on it. We have noticed an increase in magnetic moment by C/N-adsorption in G-MV as listed in Table 2. In contrast to G-MV, this moment becomes almost double/triple on C/N-adsorption. The equivalent atoms of G-MV e.g. (C_1 and C_2), (C_3 and C_4), etc., become non-equivalent on adsorption due to drastic change in local environment near to adsorption site. Now the main contribution not only comes from adsorbed C/N atom but also from these inequivalent C-atoms. However, some magnetic moment is found to be distributed even in the interstitial regions among C-atoms, which is also the case for transition metal decorated silicene. This indicates

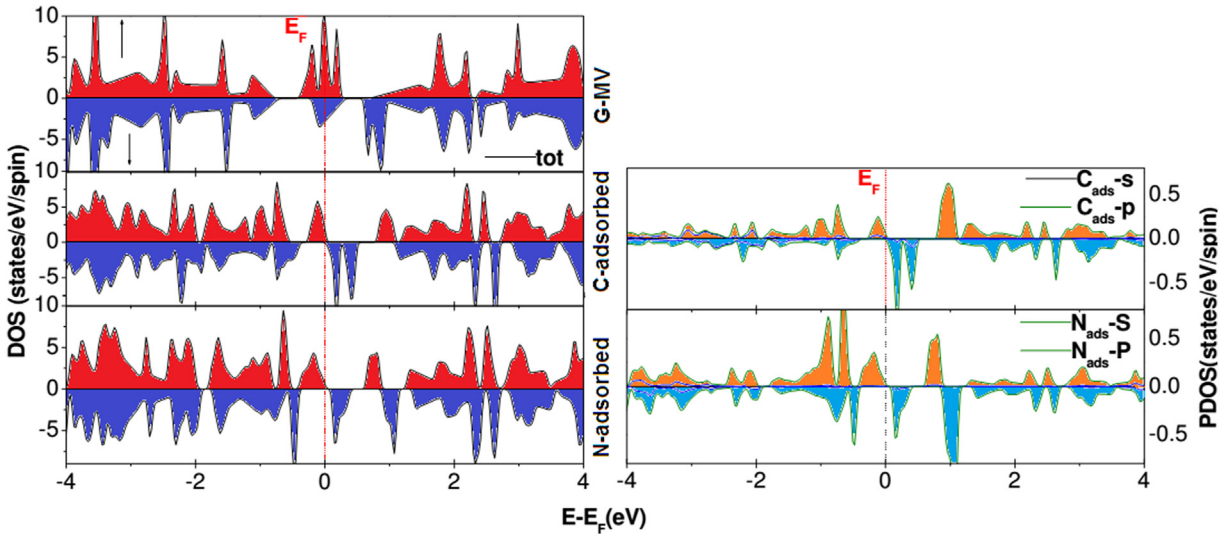

Fig. 4. TDOS of G-MV and C/N-adsorbed G-MV. The right panel shows partial DOS of adsorbed C/N atom.

Table 2
Calculated DOS of MAC and MIC (i.e. $N_{\uparrow}(E_F)$ and $N_{\downarrow}(E_F)$ in states/eV, respectively), spin-polarization (P) at E_F, electronic band gap in MIC (E_g in eV), Half metallic gap (E_{HM} in eV), observed metallic state and total magnetic moment (M_{tot} in μ_B) of pristine graphene, G-MV, C/N-adsorbed G-MV.

Graphene nanosystem	$N_{\uparrow}(E_F)$	$N_{\downarrow}(E_F)$	P (%)	E_g	E_{HM}	State	M_{tot}
Pristine case	0.00	0.00	0.0	–	–	Semi-metallic	0.00
G-MV	8.12	2.70	50.1	–	–	Metallic	0.99
C-adsorbed G-MV	2.14	0.00	100.0	0.71	0.0	Half-metallic	1.98
N-adsorbed G-MV	0.36	0.00	100.0	0.62	0.1	Half-metallic	3.11

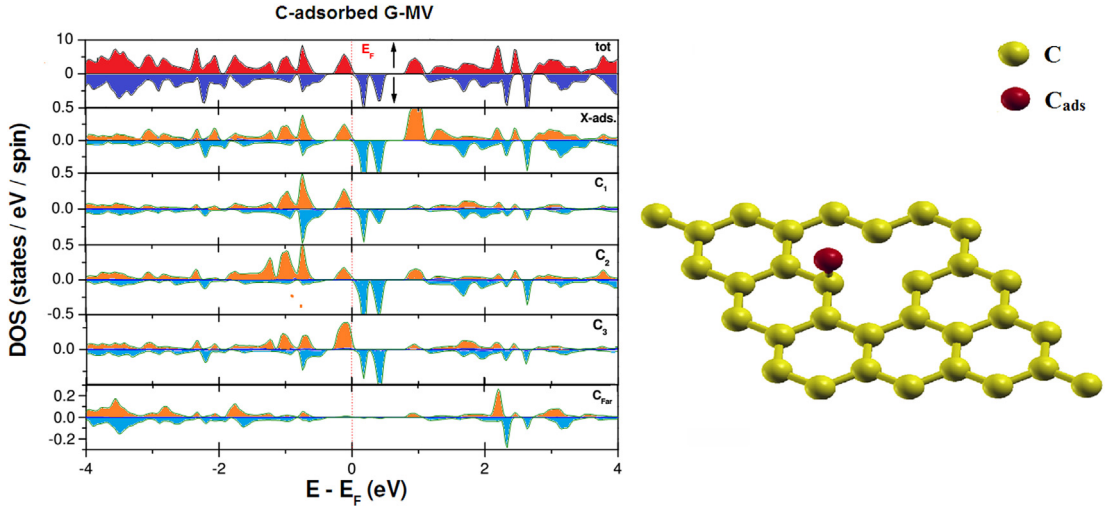

Fig. 5. Partial density of states (PDOS) and supercell used for C-adsorbed G-MV.

that the magnetic moment distributed over the interstitial regions should also have significant contribution and thus cannot be neglected [80]. The other C-atoms, which are away from dopant, do not possess significant magnetic moment even after adsorption.

The isosurface analysis clearly justifies the appearance of a particular magnetic state. To examine this, we have analyzed spin density difference isosurface for adsorption of C-atom in graphene. An isosurface is a three dimensional contour plot of the electron charge density difference, i.e. the difference of electron charge density of the C-adsorbed graphene system and that of the isolated C-atom. Fig. 6 represents the interaction of adsorbed C-atom with inequivalent C_1, C_2 and C_3 atoms (these inequivalent atoms are picturized in Fig. 2) which is maximum around the vacancy site. It reflects that the total magnetic moment is essentially contributed from the adsorbed C-atom with a tiny contribution from nearest C-atoms.

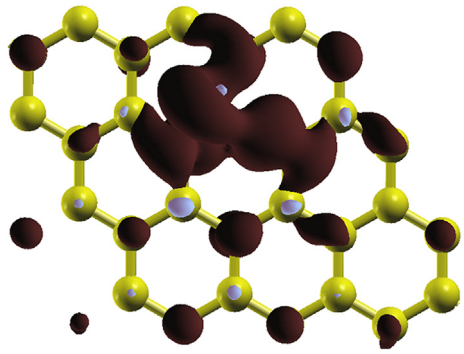

Fig. 6. Spin density difference isosurface for C adsorbed atom in $4 \times 4 \times 1$ supercell of G-MV. The isosurface corresponds to a value of 2×10^{-3}electrons/Å^3 (Brown/blue color indicates majority/minority spin component). (For interpretation of the references to colour in this figure legend, the reader is referred to the web version of this article.)

4. Conclusions

In summary, we have investigated the electronic and magnetic properties of G-MV with and without C/N-adsorption by using the first-principles calculations based on DFT. The C/N-adsorption in G-MV induces the highly spin-polarization (100%) and gives rise to magnetic moment of 1.98 μ_B/3.11 μ_B. The high degree of the spin-polarization ensures the potential use of studied nanomaterials in spin filter devices [67–69]. The enhancement of the spin-polarization and magnetism has been identified via interaction of p-states of adsorbed atom with p-states of inequivalent C-atoms, located in the vicinity of adsorption site. An appreciable band gap of <1 eV in both type of adsorption in G-MV may lead to interesting optical properties. Consequently, the study of present nanomaterials suggests that adsorption of C/N on surface of G-MV is a promising route to modify the properties of graphene and to increase its potential in future spintronic and magnetic device applications [7–9].

Acknowledgments

The computational facilities used for the work are supported by UGC, INDIA, grant No. 41-922/2012 (SR) sanctioned to M.K. Kashyap. H.S. Saini acknowledges UGC, INDIA for providing financial support as Dr. D. S. Kothari post doctoral fellowship. A.H. Reshak would like to acknowledge the CENTEM project, reg. no. CZ.1.05/2.1.00/03.0088, co-funded by the ERDF as part of the Ministry of Education, Youth and Sports OP RDI programme and, in the follow-up sustainability stage, supported through CENTEM PLUS (LO1402) by financial means from the Ministry of Education, Youth and Sports under the"National Sustainability Programme I. Computational resources were provided by MetaCentrum (LM2010005) and CERIT-SC (CZ.1.05/3.2.00/08.0144) infrastructures.

References

[1] K.S. Novoselov, A.K. Geim, S.V. Morozov, D. Jiang, M.I. Katsnelson, I.V. Griegorieva, et al., Nature 438 (2005) 197.
[2] A.K. Geim, K.S. Novoselov, Nat. Mater. 6 (2007) 183.
[3] K.I. Bolotin, K.J. Sikes, Z. Jiang, M. Klima, G. Fudenberg, J. Hone, et al., Solid State Commun. 146 (2008) 351.
[4] Y. Zhang, Y.W. Tan, H.L. Stormer, P. Kim, Nature 438 (2005) 201.
[5] M.Y. Han, B. Özyilmaz, Y. Zhang, P. Kim, Phys. Rev. Lett. 8 (2007) 206805.
[6] C. Lee, X. Wei, J.W. Kysar, J. Hone, Science 321 (2008) 385.
[7] W. Han, R.K. Kawakami, M. Gmitra, J. Fabian, Nat. Nanotechnol. 9 (2014) 794.
[8] M.V. Kamalakar, C. Groenveld, A. Dankert, S.P. Dash, Nat. Commun. 6 (2015) 6766.
[9] T. Taychatanapat, K. Watanabe, T. Taniguchi, P. Jarillo-Herrero, Nat. Phys. 9 (2013) 225.
[10] J. Thakur, H.S. Saini, M. Singh, A.H. Reshak, M.K. Kashyap, Phys. E 78 (2016) 35.
[11] D. Wang, Z. Zhang, Z. Zu, B. Liang, Sci. Rep. 4 (2014) 7587.
[12] Y. Yin, Z. Cheng, L. Wang, K. Jin, W. Wang, Sci. Rep. 4 (2014) 5758.
[13] A. Pachoud, M. Jaiswal, P.K. Ang, K.P. Loh, B. Oezyilmaz, Europhys. Lett. 92 (2010) 27001.
[14] T.P. Kaloni, Y. Cheng, M.U. Kahaly, U. Schwingenschlögl, Chem. Phys. Lett. 534 (2012) 29.
[15] T.P. Kaloni, Y. Cheng, M.U. Kahaly, U. Schwingenschlögl, Appl. Phys. Lett. 104 (2014) 073116.
[16] T.P. Kaloni, Y. Cheng, M.U. Kahaly, U. Schwingenschlögl, Europhys. Lett. 98 (2012) 67003.
[17] J.J. Palacios, J. Fernández-Rossier, L. Brey, Phys. Rev. B 77 (2012) 195428.
[18] B.R.K. Nanda, M. Sherafati, Z.S. Pobovic, S. Satpathy, New J. Phys. 14 (2012) 083004.
[19] G.O. Lee, C.Z. Wang, E. Yoon, N.M. Hwang, D.Y. Kim, K.M. Ho, Phys. Rev. Lett. 95 (2005) 205501.
[20] X. Zhang, X. Chen, K. Zhang, S. Pang, X. Zhou, H. Xu, et al., J. Mater. Chem. A 1 (2013) 3340.
[21] Y.C. Cheng, T.P. Kaloni, Z.Y. Zhu, U. Schwingenschlögl, Appl. Phys. Lett. 101 (2012) 073110.
[22] T.P. Kaloni, Y.C. Cheng, R. Faccio, U. Schwingenschlögl, J. Mater. Chem. 21 (2011) 18284.
[23] J. Thakur, M.K. Kashyap, H.S. Saini, A.H. Reshak, J. Alloys Compds 649 (2015) 1300.
[24] Y. Kim, J. Ihm, E. Yoon, G.D. Lee, Phys. Rev. B 84 (2011) 075445.
[25] A.W. Robertson, B. Montanari, K. He, C.S. Allen, Y.A. Wu, N.M. Harrison, et al., ACS Nano 7 (2013) 4495.
[26] J.E. Santos, N.M. Peres, J.M.L. Santos, A.H.C. Neto, Phys. Rev. B 84 (2011) 085430.
[27] Z. Wang, X. Niu, Q. Su, H. Deng, Z. Li, W. Hu, et al., J. Phys. Chem. C 117 (2013) 17644.
[28] O. Lehtinen, I.L. Tsai, R. Jalil, R.R. Nair, J. Keinonen, U. Kaiser, et al., Nanoscale 6 (2014) 6569.
[29] J.R. Hahn, H. Kang, Phys. Rev. B 60 (1999) 6007.
[30] R. Faccio, L.F. Werner, H. Pardo, C. Goyenola, O.N. Ventura, A.W. Mombru, J. Phys. Chem. C 114 (2010) 18961.
[31] E.J. Kan, Z. Li, J. Yang, J.G. Hou, Appl. Phys. Lett. 91 (2007) 243116.
[32] E. Rudberg, P. Salek, Y. Luo, Nano Lett. 7 (2007) 2211.
[33] J. Jung, A.H. MacDonald, Phys. Rev. B 81 (2010) 195408.
[34] G. Compagnini, F. Giannazzo, S. Sonde, V. Raineri, E. Rimmi, Carbon 47 (2009) 3201.
[35] O. Lehtinen, J. Kotakeski, A.V. Krasheninniov, J. Keinenon, Nanotechnology 22 (2011) 175306.
[36] J. Zeng, H.J. Yao, S.X. Zang, P.F. Zhai, J.L. Duan, Y.M. Sun, et al., Nucl. Inst. Meth. B 330 (2014) 18.
[37] L. Tapaszto, G. Dobrik, P. Nemes-Incze, G. Vertesy, P. Lambin, L.P. Biro, Phys. Rev. B 78 (2008) 233407.
[38] A. Ney, P. Papakonstantinou, A. Kumar, N.G. Shang, N. Peng, Appl. Phys. Lett. 99 (2011) 102504.
[39] J. Zhou, Q. Wang, Q. Sun, X.S. Chen, Y. Kawazoe, P. Jena, Nano Lett. 9 (2009) 3100.
[40] B. Xu, J. Yin, Y.D. Xia, X.G. Wan, K. Jiang, Z.G. Liu, Appl. Phys. Lett. 96 (2010) 163102.
[41] D. Xiao, W. Yao, Q. Niu, Phys. Rev. Lett. 99 (2007) 236809.
[42] R.R. Nair, M. Sepioni, I. Tsai, O. Lehtinen, J. Keinonen, A.V. Krasheninnikov, et al., Nat. Phys. 8 (2012) 199.
[43] J. Červenka, C.F.J. Flipse, Phys. Rev. B 79 (2009) 195429.
[44] P.O. Lehtinen, A.S. Foster, A. Ayuela, A.V. Krashenninnikov, R.M. Nieminen, Phys. Rev. Lett. 93 (2004) 187202.
[45] G.D. Lee, C.Z. Wang, E. Yoon, N.M. Hwang, D.Y. Kim, K.M. Ho, Phys. Rev. Lett. 95 (2005) 205501.
[46] O.V. Yazyev, L. Helm, Phys. Rev. B 75 (2007) 125408.
[47] T.P. Kaloni, Y.C. Cheng, U. Schwingenschlögl, Euro Phys. Lett. 100 (2012) 37003.
[48] M. Weinert, E. Wimmer, A.J. Freeman, Phys. Rev. B 26 (1982) 4571.
[49] G. Kresse, J. Furthmüller, Comp. Mater. Sci. 6 (1996) 15.
[50] G. Kresse, J. Furthmüller, Phys. Rev. B 54 (1996) 11169.
[51] J.P. Perdew, K. Burke, M. Ernzehof, Phys. Rev. Lett. 77 (1996) 3865.
[52] G.K.H. Madsen, P. Blabha, Phys. Rev. B 64 (2001) 195134.
[53] P. Blaha, K. Schwarz, G. Madsen, D.K.J. Luitz, Wien2k: An Augmented Plane Wave Plus Local Orbitals Program for Calculating Crystal Properties, Vienna University of Technology, Austria, 2001, ISBN 3-9501031-1-2.
[54] P.E. Blöchl, O. Jepsen, O.K. Andersen, Phys. Rev. B 49 (1994) 16223.
[55] A.M. Scott, E.A. Burns, B.J. Lafferty, F.C. Hill, J. Mol. Model. 21 (2015) 1.
[56] L. Pauling, The Nature of Chemical Bond, Cornell Univ. Press, New York, 1960.
[57] T.P. Kaloni, M.U. Kahaly, R. Faccio, U. Schwingenschlögl, Carbon 64 (2013) 281.
[58] R.P. Hardikar, D. Das, S.S. Han, K.R. Lee, A.K. Singh, Phys. Chem. Chem. Phys. 16 (2014) 16502.
[59] P.A. Thrower, R.M. Mayer, Stat. Sol. A 47 (1978) 11.
[60] G.D. Lee, C.Z. Wang, E. Yoon, N.M. Hwang, K.M. Ho, Phys. Rev. B 74 (2006) 245411.
[61] Sohee Park, Changwon Park, Gunn Kim, J. Chem. Phys. 140 (2014) 134706.
[62] T. Björkman, S. Kurasch, O. Lehtinen, J. Kotakoski, O.V. Yazyev, A. Srivastava, et

al., Sci. Rep. 3 (2013) 3482.
[63] R.J. Soulen Jr., J.M. Byers, M.S. Osofsky, B. Nadgorny, T. Ambrose, S.F. Cheng, et al., Science 282 (1998) 85.
[64] H.S. Saini, M. Singh, A.H. Reshak, M.K. Kashyap, Comp. Mat. Sci. 74 (2013) 114.
[65] M. Singh, H.S. Saini, M.K. Kashyap, J. Mater. Sci. 48 (2013) 1837.
[66] A.W. Robertson, B. Montanari, K. He, C.S. Allen, Y.A. Wu, N.M. Harrison, et al., ACS Nano 7 (2013) 4495.
[67] V.M. Karpan, G. Giovannetti, P.A. Khomyakov, M. Talanana, A.A. Starikov, M. Zwierzycki, et al., Phys. Rev. Let. 99 (2007) 176602.
[68] X.H. Zheng, R.N. Wang, L.L. Song, Z.X. Dai, X.L. Wang, Z. Zeng, Appl. Phys. Lett. 95 (2009) 123109.
[69] W. Sheng, Z. Ning, Z.Q. Yang, H. Guo, Nanotechnology 21 (2010) 385201.
[70] G. Kim, S.H. Jhi, S. Lim, N. Park, Appl. Phys. Lett. 94 (2009) 173102.
[71] Y. Wang, Y. Feng, G. Meng, X. Dong, X. Huang, Phys. Status Solidi B 252 (2015) 1757.
[72] P. Johari, V.B. Shenoy, ACS Nano 5 (2011) 7640.
[73] Y. Noguchi, S. Osamu, J. Chem. Phys. 142 (2015) 064313.
[74] B.G. Lui, Phys. Rev. B 67 (2003) 172411.
[75] W.H. Xie, Y.Q. Xu, B.G. Liu, D.G. Pettifor, Phys. Rev. Lett. 91 (2003) 037204.
[76] N. Tombros, C. Jozsa, M. Popinciuc, H.T. Jonkman, B.J. van Wees, Nature 448 (2007) 571.
[77] H. Haugen, H.H. Daniel, A. Brataas, Phys. Rev. B 77 (2008) 115406.
[78] T. Yokoyama, Phys. Rev. B 77 (2008) 073413.
[79] B. Dlubak, M.B. Martin, C. Dermlot, B. Servet, S. Xavier, R. Mattana, et al., Nat. Phys. 8 (2012) 557.
[80] T.P. Kaloni, N. Singh, U. Schwingenschlögl, Phys. Rev. B 89 (2014) 035409.